JOURNAL OF AIRCRAFT
Vol. 46, No. 5, September–October 2009

Conceptual Design Prediction of the Buffet Envelope of Transport Aircraft

Adrien Bérard*
Royal Institute of Technology, 100 44 Stockholm, Sweden
and
Askin T. Isikveren†
University of Bristol, Bristol, England BS8 1TR, United Kingdom

DOI: 10.2514/1.41367

This paper describes a methodology that inexpensively predicts the buffet envelope of new transport airplane wing geometries at the conceptual design stage. The parameters that demonstrate a strong functional sensitivity to buffet onset were identified and their relative effect was quantified. To estimate the buffet envelope of any target aircraft geometry, the method uses fractional change transformations in consort with a generic reference buffet onset curve provided by the authors or the buffet onset of a known seed airplane. The explicit design variables required to perform buffet onset prediction are those describing the wing planform and the wingtip section. The mutually exclusive nature of the method's analytical construct provides considerable freedom in deciding the scope of free-design-variable complexity. The method has been shown to be adequately robust and flexible enough to deal with a wide variety of transport airplane designs. For the example transport airplanes considered, irrespective of aircraft morphology and en route flight phase, the relative error in prediction was found to be mostly within ±5.0%, with occasional excursions not exceeding a ±9.0% bandwidth. The standard error of estimate for the lift coefficient at 1.0 *g* buffet onset at a given Mach number was calculated to be 0.0262.

Nomenclature

AR	=	reference wing aspect ratio
a	=	arbitrary coefficient of proportionality or exponent
b	=	arbitrary coefficient of proportionality or exponent
b	=	wingspan, m or ft
C_L	=	operating lift coefficient
C_{LB}	=	lift coefficient at the onset of 1.0 g buffet for a given Mach number
$\tilde{C}_{LB}$	=	lift coefficient at the onset of 1.0 g buffet decoupled from the influence of reference wing taper ratio
c	=	wing section camber, m
c	=	local wing planform chord length, ft
k_n	=	constant of proportionality or exponent that establishes a relationship between flow regime, primary wing design variables, and the maximum permissible operating lift coefficient at buffet onset for a given Mach number
M	=	Mach number
$\tilde{M}$	=	Mach number at the onset of 1.0 g buffet decoupled from the influence of reference wing sweep
M_B	=	Mach number at the onset of 1.0 g buffet for a given attainable lift coefficient
S_W	=	reference wing area, m^2 or ft^2
t/c	=	wing section thickness-to-chord ratio at a given wing spanwise buttock line or at the wingtip
W	=	all-up weight, kg
W	=	instantaneous gross weight, lb
X	=	longitudinal position along wing section from leading-edge datum, normalized by chord length
x_n	=	arbitrary independent or dependent variable or design parameter
α	=	exponent that establishes a relationship between wing sweep and the maximum permissible operating lift coefficient at buffet onset for a given Mach number
β	=	exponent that establishes a relationship between wing section thickness-to-chord ratio and the maximum permissible operating lift coefficient at buffet onset for a given Mach number
γ	=	exponent that establishes a relationship between wing section camber and the maximum permissible operating lift coefficient at buffet onset for a given Mach number
ε	=	error function, applicable for absolute or relative values
η	=	given wing spanwise buttock line normalized by wing semispan
Θ	=	generic function representing the buffet onset of an unswept taper ratio of unity flat-plate representation of a wing
ϑ	=	constant of proportionality that establishes a relationship between wing section camber and the maximum permissible operating lift coefficient at buffet onset for a given Mach number
κ	=	linear correlation used for establishing wing thickness-to-chord sensitivity to operating lift coefficient at buffet
Λ	=	reference wing sweep, rad or deg
λ	=	taper ratio for individual trapezoidal panel, original or reference wing taper ratio
ξ	=	set of ancillary design parameters that influence the maximum permissible operating lift coefficient at buffet onset for a given Mach number
ρ	=	ambient density at altitude, kg/m^3 or $slugs/ft^3$
τ	=	constant of proportionality that establishes a relationship between wing sweep and the maximum permissible operating lift coefficient at buffet onset for a given Mach number
Ω	=	generic function representing the influence of ancillary design parameters on the maximum permissible operating lift coefficient at buffet onset for a given Mach number

Received 6 October 2008; accepted for publication 11 May 2009.

*Ph.D. Candidate, Department of Aeronautical and Vehicle Engineering. Member AIAA.

†Director, Engineering Design and Integrated Systems Design, Department of Aerospace Engineering. Member AIAA.

ω	=	constant of proportionality that establishes a relationship between wing section thickness to chord and the maximum permissible operating lift coefficient at buffet onset for a given Mach number
Δ	=	incremental change in a parameter or design variable
$\triangleleft$	=	fractional change operator, incremental change in parameter normalized by original value

Subscripts

AREF	=	alternate reference wing standard pertaining to wing geometric definition
act	=	actual value used as data set point for nonlinear regression
dats	=	data set used for nonlinear regression analysis
ESDU	=	Engineering Science Data Unit reference wing standard pertaining to wing geometric definition
est	=	estimated value based on nonlinear regression analysis
exp	=	exposed wing planform geometry (i.e., outboard from the wing–fuselage juncture)
gen	=	generic reference wing standard pertaining to a 1.0 g buffet onset envelope
hchd	=	half-chord locale pertaining to reference wing sweep
MO	=	maximum operating condition associated with Mach number
n	=	number of elements in a data set, trapezoidal panel number, natural number
o	=	original wing planform geometry
qchd	=	quarter-chord locale pertaining to reference wing sweep
R	=	wing root locale
ref	=	reference condition or aircraft
SEE	=	standard error of estimate
T	=	wingtip locale
t/c max	=	line of maximum section thickness pertaining to reference wing sweep
tgt	=	target condition or aircraft
WF	=	wing–fuselage juncture pertaining to quantification of chord length
0	=	seed or starting parameter condition
1	=	new or target parameter condition
2-D	=	two-dimensional representation or transformation

I. Introduction

THE primary objective of transport aircraft initial sizing during the conceptual design or initial technical assessment phase is to produce a tentative engineering proposal that meets the requirements of a current (or envisioned) market niche with facility for accommodating perceived future needs constrained by the realities of contemporary and foreseeable economic forces. To compound the original problem statement, conceptual designers also endeavor to meet the often-challenging goal of generating a so-called balanced design: one in which most or all the critical cases converge into a single solution for sizing. Specifically, the solution is conditioned in such a manner that when one critical case is removed from the design driver matrix, the remaining active critical cases promote a sizing result similar, if not identical, to the original hyperconstrained synthesized solution. The analytical processes that aid in bringing a conceptual design into fruition are primarily based on methods that are simple (to, at most, moderately high) in complexity; in this way, minimizing the level of expense required in performing predictions is at a premium.

Current industrial trends indicate that the universal theme for transport aircraft integrators is to employ a time-zero family concept tempered by the practice of mostly conventional design morphology. Generally, an aircraft family comprises all or some of the following elements: baseline or "clean-sheet" aircraft, variant(s), and derivative(s).

An aircraft variant is taken to be the development of a new aircraft product from an original baseline or clean sheet via the increase (or decrease) of maximum takeoff weight and incorporation of enhancements through any equipment and/or amenities upgrade; most important, it does not generate any changes to the baseline aircraft outer mold lines (OMLs). Derivatives involve the creation of a new aircraft product that not only incorporates any or all of the attributes that constitute an aircraft variant but also generates alterations to the baseline aircraft OMLs through a fuselage stretch/shrink, wing and empennage geometric modifications, or powerplant system changes. In this respect, there is now an ever-increasing tendency to envisage variant and derivative aircraft concurrently with the intention of the offerings being strategically introduced over time, eventually replacing an aging product line or targeting a new market segment once maturity has been established for the baseline.

The focal point that emerges from analyzing systems, structures, weights balance, aerodynamics, and propulsion characteristics of a vehicle candidate is the operational performance technical subspace. During aircraft product-development critical appraisals this aspect is considered to be crucial, because it is used as a fundamental comparison basis not only in an absolute sense but also when transformed into the cash operating cost (COC) or direct operating cost (DOC) functional forms. From an operational perspective, one important measure that significantly influences the integrated efficiency and/or productivity of an aircraft is altitude capability or highest altitude achievable at a given forward speed and all-up weight. Altitude capability is limited by one of two conditions: engine thrust limit or aerodynamic buffet margin.

The buffet envelope constitutes one of the primary constraints in establishing the low-to-intermediate and high-speed en route performance capabilities of transport aircraft. The physical phenomenon of buffet is defined as excitation imposed on a structure because of separated airflow, with the subsequent vibration (or buffeting) directly attributable to the response of the structure. This vibration, particularly when it concerns the flexible modes of the structure, can have a strong influence on aircraft aerodynamic performance and when left unchecked leads to structural damage or even catastrophic failure. The buffet envelope is presented as an airplane flight-manual limitation defined by flight test, and the onset (at 1.0 g condition) is typically identified as the speed at which the vibration reaches ± 0.050 g while windup turns at constant Mach are executed. Although it is a certified operational constraint, the 1.0 g buffet onset is not taken to be a strict physical limit to the actual flight envelope of the aircraft; it basically sets a boundary between a safe flight domain and a flight domain in which the flight crew may encounter serious control problems and/or the aircraft is prone to severe instantaneous or fatigue loads. Because the buffet is the result of flow separation, the wing is usually its primary cause; however, buffet can arise from localized flow separation emanating from other locales of the aircraft (e.g., the fuselage), but this is considered to be quite rare. Finally, the aerodynamic buffet margin defines the extent of maneuver capability during flight, and thus the buffet boundary is declared as a limitation that influences the actual operating flight envelope. Operational regulations stipulate a margin of 0.30 g in smooth air (i.e., equivalent to a 40 deg bank angle while maintaining level flight). Additional operator specific requirements would also include maneuver capability through moderate turbulence (e.g., penetration with 0.50 g margin).

Design intent is to ensure that en route climb capability is not unduly limited by intermediate-speed aerodynamic buffet restrictions (i.e., the desire is to achieve a balance with thrust limited performance) in achieving the COC or DOC optimum initial cruise altitude. Correspondingly, COC or DOC optimal flight techniques involving an intermediate-speed descent schedule could become prohibitive, because buffet limitations could lead to a flight profile that restricts the final cruise segment altitude to a lower one. An additional requirement is to ensure that the high-speed buffet envelope is sufficiently broad such that it does not curtail the aircraft maximum operating Mach number (M_{MO}) capability. A substantial mismatch between M_{MO} and the buffet boundary would, in some instances, limit the ability of an aircraft to reduce COC and DOC,

maximize productivity, improve on-time dependability, or even thwart the ability of conducting an all-important emergency descent flight-technique target. Therefore, good design practice requires that M_{MO} should not to be overly limited by buffet during such critical phases of flight. Finally, in an effort to reduce wing planform size and corresponding thrust requirements, increasing emphasis is placed upon producing expanded buffet boundaries. This philosophy becomes rather important when family concepts comprising increased gross weight variants/derivatives are synthesized concurrently.

The conceptual design phase is typified by the sizing of a multitude of design candidates generated by the need to conduct a voluminous array of technical feasibility or trade studies under the limits of compressed timelines. This means that relatively simple prediction tools must demonstrate characteristics of conformity, robustness, consistency, and applicability for the design problem at hand, with emphasis being placed upon an appropriate functional sensitivity to the free design variables. Another important consideration is the ability for any designer/analyst to gauge the sensitivity of primary drivers almost instantaneously; that is, the array of sensitivities will need to be presented in a fashion that is open to rapid interpretation. By ensuring that the level of conformity of these highly simplified and expedient prediction methods does not breach an error bandwidth of $\pm 5.0\%$, it can also function as an all-important reference point to check the continued validity of more sophisticated level of analyses as the project work matures.

In an attempt to fulfill the preceding criteria, the extent of sophistication of traditional conceptual design methods is the adoption of the buffet envelope of an actual or sufficiently mature paper aircraft that closely matches the parametric attributes of the target design candidate. Apart from the inability to perform sensitivity or trade studies beyond inspection of the reference wing area S_W (or, indirectly, wing loading W/S_W), a common problem is finding an appropriately matching envelope for a target design candidate that attempts to service an unfamiliar mission role or an untried market segment.

To permit greater design freedom, a more advanced variation used by industry that permits a limited scope for design sensitivity studies is offered in [1]. The process is outlined in the flowchart presented in Fig. 1. It is highlighted that the method given by [1] attempts to promote physical compatibility by using Λ_{hchd} as a basis for 3-D $\leftrightarrow$ 2-D transformations (simple sweep theory [3]) as opposed to the more familiar Λ_{qchd}, because the formation of any weak or strong shocks generally occurs closer to wing half-chord locales.

Another semi-empirically-based method given by [3] is described in the flowchart given in Fig. 2.

Industrial practice usually relies upon a hybrid of the preceding utilitarian method with more advanced numerical aerodynamic analysis methods. In design offices, suitably tuned high-end low-fidelity (such as transonic small disturbance) and high-fidelity computational fluid dynamics (CFD) codes would be executed to predict the 1.0 g buffet onset of the target aircraft. In addition, sensitivity studies using CFD analysis methods would help to establish the requisite linear factor in the incremental t/c sensitivity model of Eq. (1) as given by [1]. Coupled CFD and computational structural dynamics can also be used; however, it is a time-consuming exercise in terms of problem setup and proves to be computationally expensive.

An even more elaborate method of predicting 1.0 g buffet onset is to use wind-tunnel-generated experimental results, but this is known to be relatively inaccurate. The reason is due to three aspects: first, the wind-tunnel-borne results need to be extrapolated to full scale; second, buffet onset can be masked by the level of flow unsteadiness in the wind tunnel; and third, the wind tunnel allows one to record flow separation and model vibration, whereas the dynamic structural properties of the actual aircraft produce buffeting. Finally, the ultimate way to establish the buffet onset is through flight testing, but this is an unrealistic option during the conceptual design stage of analysis.

The purpose of this paper is to present a method that facilitates relatively advanced semi-empirical functional sensitivities to compute the variations of 1.0 g buffet onset when the geometry of a wing, for which the buffet onset is known, is modified. The concern of this study is also to highlight the design parameters for which the influence on buffet is relevant and is traditionally known or studied at the conceptual design stage. This work is based upon fractional change theory [4] and hence provides the advantage of instantaneous interpretation of functional sensitivity with respect to relative variations of wing geometry. Although the use of fractional change theory is founded on the underlying premise that the designer begins with a known aircraft, a generic reference curve will also be derived and can be used in the absence of a known, or seed, buffet envelope.

II. Buffet Prediction Algorithm Synthesis

Conceptual design prediction methods rely predominately on semi-empirical constructs generated from nonlinear regression techniques. The unfortunate characteristic of such methods is that they

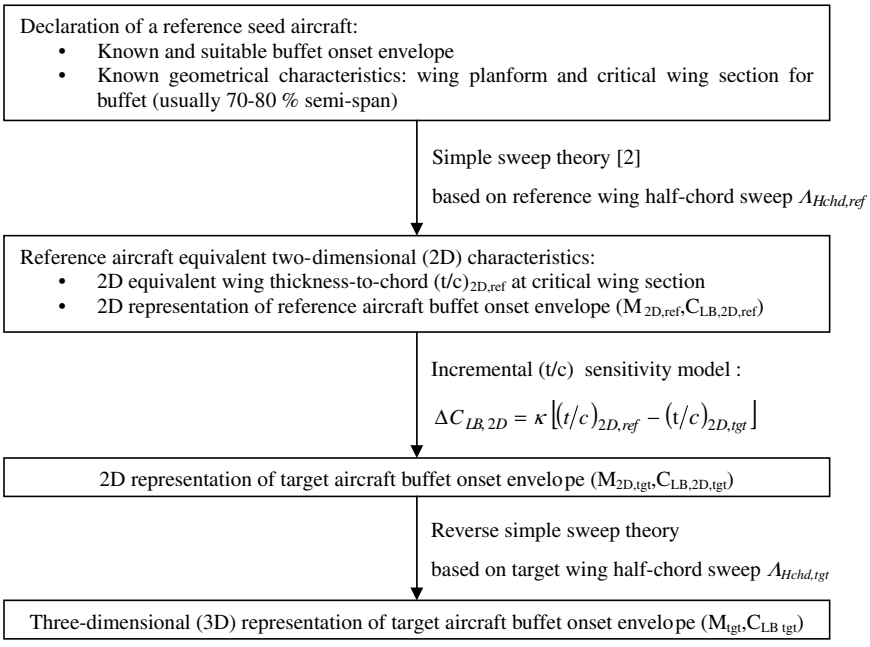

Fig. 1 A semi-empirical buffet onset prediction method used by industry [1].

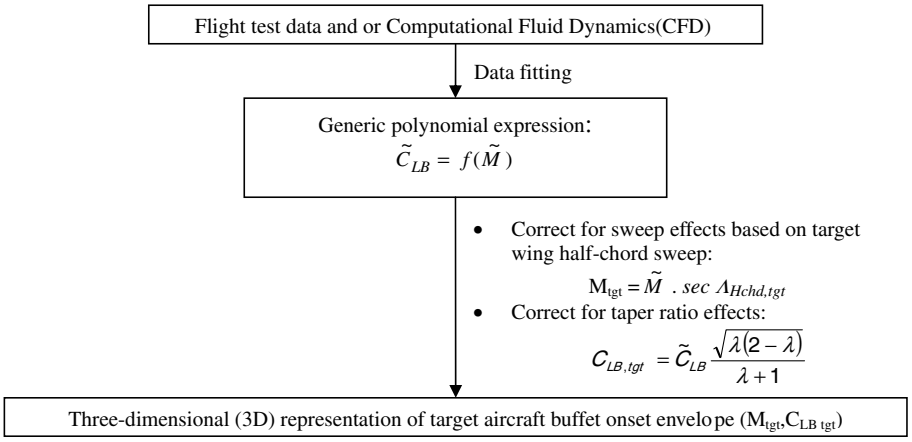

Fig. 2 A second semi-empirical buffet onset prediction method used by industry [3].

can only be considered to be a curve fit of historical data sets, which imposes restrictions on the degree of applicability when coupled into multidisciplinary design optimization suites. To establish applicability of newly procured conceptual design methods suitable for implementation in an automated-sizing environment, the authors have formulated a set of guidelines. To this end, six tenets that would constitute legitimate declaration of a useful and flexible mathematical model are proposed as follows:

1) Consistency: the analytical construct adheres to a sound physical and theoretical model.

2) Scope: the number of free design variables that permit functional sensitivity is maximized.

3) Transparency: the sensitivity of primary design drivers is gauged in a rapid manner.

4) Conformity: the model is able to predict effectively within the bounds of the original data set, but adequate performance should also be exhibited when employed outside the bounds of the training data set.

5) Robustness: the model is able to predict effectively up to a predetermined level of design-related uncertainty or aircraft morphological variation.

6) Malleability: inherently flexible prediction algorithms allow the best mix of generic and in-house-developed subtier methodologies.

A. Buffeting Physical Mechanisms and Behavior

To formulate a theoretically coherent mathematical model (i.e., address the modeling tenets of consistency and scope), a review paper published by Mabey [5] was used. It is highlighted that the review paper summarizes a series of observations and conclusions derived from systematic buffet measurements conducted by Ray and Taylor [6] of NASA on a series of 11 swept wings mounted atop a simple fuselage. A qualitative review of wing design parameter sensitivity was based on experimental results derived from this single morphology having combinations of aspect ratio AR $\in [4.0 \quad 5.0 \quad 6.0]$, quarter-chord sweep $\Lambda_{\text{qchd}} \in [25 \quad 35 \quad 45\,\text{deg}]$, and associated camber c and position of maximum thickness $X_{t/c\,\max}$ for NACA 63A006/08, 63A208, 63A408, 63A010, 64A010, and 65A006/08 sections. Inspection of these parametric interval values indicate some inconsistency with regard to typical transport aircraft sizing (namely, aspect ratios usually greater than 7.0), and t/c generally have a minimum value of around 0.10. Irrespective of this, the physical observations were construed as being useful for the ensuing buffet onset model-development work, because they enabled definition of the proposed model scope.

As expounded earlier, buffet is the aerodynamic excitation of the structure due to separated flow and, as a result, is closely linked to the Mach number, the angle of attack, and the geometry of the wing. For a given wing geometry, the 1.0 g buffet onset locus is commonly represented using a C_{LB}-vs-M graph (see Fig. 3), implicitly showing the relative influence of the angle of attack. Figure 3 illustrates that there are three distinct zones that describe the onset curve, each of which is characterized by the type of separation taking place. For subsonic speeds, usually $\leq M = 0.50$, C_{LB} drops at a docile rate with increasing Mach number, because buffet onset is due to leading-edge flow separation. Decreasing values of C_{LB} are associated with higher Mach numbers, because an increasing pressure gradient is generated by virtue of compressibility effects in the leading-edge region. At low-transonic speeds (approximately $M = 0.50$–0.75), the rate decrease in C_{LB} with Mach number becomes slightly more pronounced and then begins to abate with increasing speed. The primary cause of this phenomenon is the fact that flow separation can be either leading-edge or shock-induced separation or a combination of the two. The mixed-separation regime is a product of a complex 3-D shock system that promotes transonic attachment exemplified by upstream movement of the initial separation point (pronounced reduction in C_{LB} with increasing Mach number), with further increases in Mach number promoting separation downstream (benign reduction in C_{LB} with increasing Mach number due to flow reenergization). At midtransonic speeds (over approximately $M = 0.75$), flow separation is primarily due to the presence of a strong shock on the wing, and this shock spreads quickly, which explains the sudden drop of the buffet onset curve.

Figure 3 indicates that the C_{LB} locus can become quite complex in nature; that is, multiple inflexion points may inhibit reaching an adequate level of conformity when performing a nonlinear regression exercise. In an effort to examine the merits of an alternative representation, the product $C_{LB}M^2$ was also considered as the primary modeling function in a representation versus M. Although the $C_{LB}M^2$-vs-M functional relationship exhibits desirable geometric variation due to the absence of pronounced inflexions and the existence of only one stationary point (inverted parabola), narrowness of the coffin corner vertex zone (a condition in which no

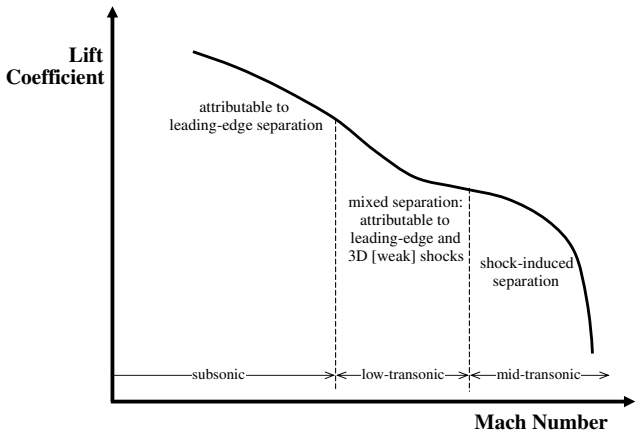

Fig. 3 Typical buffet onset curve and separation mechanisms defining the boundaries.

speed margin is available between low-speed and high-speed buffet onset) proves to be a difficult regression exercise, and thus such a relationship was rejected in favor of a more straightforward C_{LB}-vs-M relationship.

B. Sensitivities and Models Generated from Physical-Experimental Work

Before constructing predictive semi-empirical algorithms, the edicts underlying the establishment of model consistency and conformity hinge upon mimicking intrinsic behaviors displayed in experimental and/or flight-test results. Mabey [5], in his review of NASA wind-tunnel measurements, presented c, t/c, L_{qchd}, $X_{t/c\,\max}$, and aspect ratio as pertinent wing design parameters. The taper ratio λ was not explicitly investigated by Mabey; however, the authors highlight that this is a relevant parameter as well. It is appreciated by the authors that local wing incidence plays a role; nonetheless, it can be rationalized that synchronicity exists between wing section camber and local incidence angle and thus can be rolled up in the geometrical design. Furthermore, local incidence variation is usually not defined during the conceptual design stage and would be considered to be a level of detail at which the reduction in economy of effort does not trade beneficially against improvement in conformity. The subsections to follow review the sensitivity exhibited by each of the preceding six wing design variables in physical observations and propose suitable mutually exclusive analytical constructs to be later consolidated into a global buffet onset model.

1. *Influence of Primary Wing Design Variables*

Wind-tunnel experimental results presented by Mabey [5] and Ray and Taylor [6] in conjunction with the modeling results obtained for this work (presented in Sec. III, "Presentation of a Practical Buffet Onset Prediction Tool") allows one to build a notional understanding of the influence that Λ, t/c, and c have, in a mutually exclusive sense, on the buffet onset curve. Figure 4 shows that increasing Λ tends to expand the curve toward higher Mach numbers for a given C_{LB} within the midtransonic regime but tends to lower the maximum permissible C_{LB} at subsonic and low-transonic speeds. For subsonic speeds at which the buffet is due to leading-edge separation, an increased level of Λ lowers the buffet envelope because the wing section effective leading-edge radius is reduced, thereby promoting an increase in the local adverse pressure gradient, and thus increases the propensity for leading-edge-related separation. In contrast, for transonic speeds at which the buffet onset is due to shock-induced separation, increasing Λ expands the boundary because it increases the 3-D character of the shock and thus weakens it. Figure 4 also shows that an increase in t/c broadens the buffet envelope toward higher C_{LB} for a given Mach number at subsonic speeds, whereas it draws in the curve for speeds within the midtransonic regime. This is explained by the fact that the effective leading-edge radius increases with greater values of t/c, serving to delay leading-edge separation.

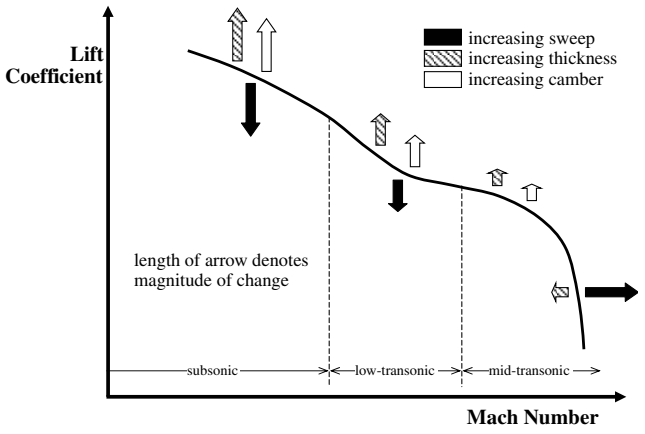

Fig. 4 Effect of a change in wing sweep; thickness-to-chord ratio and camber to the buffet onset curve.

At midtransonic speeds, an increase of t/c lowers the buffet boundary because the shock forms earlier and is strengthened, leading to an earlier separation of the flow. Finally, Fig. 4 also illustrates that increasing c expands the entire curve toward higher C_{LB} values for a given Mach number. Indeed, for subsonic speeds, increasing c reduces the adverse pressure gradient in the wing section leading-edge region, thus delaying the onset of leading-edge-related separation. For transonic speeds, [5] indicated that the development of the 3-D flow did not lead to the identification of a definitive trend; however, experimentation done by the authors using actual aircraft 1.0 g buffet onset data has lead to the conclusion that a neutral-to-minor expansion of the locus generally occurs.

2. *Modeling the Influence of Maximum Thickness Locale, Aspect Ratio, and Taper Ratio*

Shifting the wing section $X_{t/c\,\max}$ aft leads to an increase of the subsonic buffet boundary and a shrinking of the curve toward lower Mach numbers for a given C_{LB} within the midtransonic regime, because it tends to increase the wing section effective leading-edge radius, thereby reducing the local adverse pressure gradient. At transonic speeds, no universal trend was identified by Mabey [5]. Based upon such empirical observations, functional sensitivity between $X_{t/c\,\max}$ and buffet onset would be desirable; however, it can be reasoned that $X_{t/c\,\max}$ is not a typical primary design variable from the perspective of conceptual-stage sizing. In an attempt to address the requirement of scope for model formulation and accepting the notion that opportunity for refined technical assessment activities should be available (e.g., introduction of specialized aerodynamic optimization in the conceptual design loop), an indirect method to account for altering the position of $X_{t/c\,\max}$ can be incorporated via the straight trapezoid geometric relation:

$$\Lambda_{t/c\,\max} = \tan^{-1}\left[\tan\Lambda_{\text{qchd}} + \frac{4}{\text{AR}}\left(\frac{\lambda-1}{\lambda+1}\right)(X_{t/c\,\max} - X_{\text{qchd}})\right] \quad (1)$$

where X_{qchd} represents the longitudinal locale of the wing quarter-chord (i.e., $X_{\text{qchd}} = 0.25$).

Equation (1) indicates that if $X_{t/c\,\max}$ is increased, $\Lambda_{t/c\,\max}$ will decrease accordingly if $\lambda < 1.0$ for a given Λ_{qchd}, aspect ratio, and λ. This parametric relationship suitably mimics the intrinsic behavior observed in physical experimentation and thus fulfills the edict of model consistency. Reference [5] cited that increases in aspect ratio tend to expand the buffet envelope for subsonic speeds, whereas a contraction of the onset curve occurs in the transonic regime. It is argued that the shock system at transonic speeds tends toward the limit of an infinite swept wing (quasi-2-D characteristics) with greater aspect ratio: a series of lambda shocks of varying strength consolidate into a single strong shock of constant strength. Although it would have been desirable to declare aspect ratio as a conspicuous design driver in the final buffet onset model construct, indirect association using the geometric relation given by Eq. (1) was deemed to be satisfactory. Inspection of the reciprocal relationship between aspect ratio and $\Lambda_{t/c\,\max}$ as presented in Eq. (1) indicates that consistency is also satisfied from the perspective of physical-experimental observations. An interesting byproduct of using Eq. (1) is the indirect influence of λ with respect to the buffet onset functional sensitivity matrix. It can be observed that for fixed Λ_{qchd}, aspect ratio, and $X_{t/c\,\max}$, an increase in λ produces a corresponding increase in $\Lambda_{t/c\,\max}$ and is hence expected to lower the buffet boundary at subsonic speeds and expand it at transonic speeds. At the time of compiling this paper, literature verifying the association between λ and buffet onset through physical experimentation had not been found.

3. *Modeling the Influence of Sweep*

Physical-experimental results indicate that for subsonic speeds, increasing Λ lowers the buffet boundary, whereas for transonic speeds, increasing sweep raises the buffet boundary. This physical observation can be suitably modeled via an association construct

raised to an exponent, which exhibits positive and negative values corresponding to a physical change from leading-edge to weak-shock-induced separation. At a given Mach number, C_{LB} is proposed as being suitably modeled using

$$C_{LB}(\xi, \Lambda_{t/c\,\max})|_M = \Omega(\xi)(1 + \tau\Lambda_{t/c\,\max})^{\alpha} \tag{2}$$

The function $\Omega(\xi)$ represents the influence of ancillary wing design parameter quantities (namely, t/c and c) that, in consort, define the buffet boundary. A constant of proportionality τ is incorporated to facilitate a direct relationship between $\Lambda_{t/c\,\max}$ and C_{LB}. The exponent α needs to exhibit functional sensitivity with Mach number; assuming a linear relationship of the form

$$\alpha = k_1 + k_2 M^{k_3} \tag{3}$$

Upon quantification of coefficients k_1, k_2, and k_3, a test of physical significance and hence establishment of algorithm consistency can be performed by inspecting the Mach number threshold at which the pure leading-edge separation changes over to a 3-D weak-shock-induced separation. This can be identified by solving for Mach numbers at the condition $\alpha = 0$.

4. *Modeling the Influence of Thickness-to-Chord Ratio*

Empirical observations indicate that the buffet boundary for subsonic flight is raised with increasing t/c, due to a reduction in the adverse pressure gradients around the leading-edge region. At transonic speeds, strengthening of shocks promotes earlier separation, thereby lowering the buffet boundary. A candidate model comprising an association construct raised to an exponent β was considered to be relevant. At a given Mach number, C_{LB} is proposed as being suitably modeled using

$$C_{LB}(\xi, t/c)|_M = \Omega(\xi)[1 + \omega(t/c)]^{\beta} \tag{4}$$

The function $\Omega(\xi)$ represents the influence of ancillary design parameter quantities (namely, $\Lambda_{t/c\,\max}$ and c) that, in consort, define the buffet boundary. The constant of proportionality ω has the requirement of swapping sign to model the Mach number threshold at which the phenomenon of mixed leading-edge and 3-D weak-shock-induced separation changes over to purely-shock-induced separation for low-to-midtransonic speeds. To serve this purpose, a linear relationship has been adopted:

$$\omega = k_4 + k_5 M^{k_6} \tag{5}$$

Upon quantification of coefficients k_4, k_5, and k_6, a test of physical significance (and hence establishment of algorithm consistency) can be performed by inspecting the Mach number threshold at which the 3-D weak shock system changes over to a strong-shock-induced separation. This can be identified by solving for Mach numbers at the condition $\omega = 0$.

5. *Modeling the Influence of Camber*

Mabey [5] stated that for subsonic Mach numbers, a reduction in adverse pressure gradients in the leading-edge region leads to an expansion of the buffet boundary with positive increments of wing section c. A candidate model comprising an association construct raised to an exponent γ was considered to be relevant. At a given Mach number, C_{LB} is proposed as being suitably modeled using

$$C_{LB}(\xi, c)|_M = \Omega(\xi)(1 + \vartheta c)^{\gamma} \tag{6}$$

The function $\Omega(\xi)$ represents the influence of ancillary design parameter quantities (namely, $\Lambda_{t/c\,\max}$ and t/c) that, in consort, define the buffet boundary. The constant of proportionality ϑ establishes a relationship between wing section camber and the maximum permissible operating lift coefficient at buffet onset for a given Mach number.

C. Concept of Fractional Change Transformations

The analytical approach in procuring a new buffet-envelope prediction method operates with an underlying premise that the designer/analyst begins with a seed or reference aircraft. Known as fractional change analytical constructs, prediction of minimum goals for variations away from the seed aircraft can then be conducted once a basic list of fundamental design variables and intermediary implicit/explicit functions are known. A significantly expanded array of formulations developed by Isikveren [4] includes a suite of fractional change algorithms covering atmospheric and general properties as well as five technical subspaces: geometric characteristics, weights, low-speed and high-speed aerodynamics, engine performance, and integrated operational performance.

As stated previously, the analytical foundation of the fractional change method assumes that the designer/analyst begins with a seed condition/aircraft. By considering an increment in variable x as $\mathrm{d}x$ or Δx, a fractional change to a new value x_1, small or otherwise, from a seed parameter x_0 is defined as

$$\triangleleft x = \frac{\Delta x}{x_0} = \frac{x_1 - x_0}{x_0} \tag{7}$$

Equation (7) has the property of quantifying a relationship between the initial condition and any subsequent variations, which can be used to derive solutions with less effort. A special set of rules of operation must be defined to execute a treatment of functional transformations [4].

D. Semi-Empirical Buffet Onset Model Construct

By using fractional change theory and starting from the buffet onset of a seed aircraft, the prediction of the buffet onset boundary of a new wing geometry is accomplished in three distinct stages summarized in Fig. 5.

The three stages of the method are described in more detail in the following steps, in which the index 0 refers to the geometry of the seed wing (for which the buffet onset is known) and index 1 flags the new target wing geometry (for which the buffet onset is to be predicted).

In addition, to elucidate the different steps of the method, consider the example of a target fictitious regional jet with the characteristics presented in Table 1.

The example seed to be used is to be a long-haul wide-body aircraft for which the geometrical characteristics are given in Table 2, and the 1.0 g buffet onset of this seed aircraft is assumed to be known.

1. *Two-Dimensional Transformation*

Initially, using simple sweep theory, the 3-D buffet onset (M_{B0}, C_{LB0}) and the reference section of the seed wing are transformed into a 2-D representation through consideration of $\Lambda_{t/c\,\max\,@T0}$:

$$M_{B0,2\mathrm{D}} = M_{B0} \cos \Lambda_{t/c\,\max\,@T0} \tag{8}$$

$$C_{LB0,2\mathrm{D}} = C_{LB0} \sec^2 \Lambda_{t/c\,\max\,@T0} \tag{9}$$

$$(t/c)_{T0,2\mathrm{D}} = (t/c)_{T0} \sec \Lambda_{t/c\,\max\,@T0} \tag{10}$$

$$c_{T0,2\mathrm{D}} = c_{T0} \sec \Lambda_{t/c\,\max\,@T0} \tag{11}$$

For the target wing geometry, a 2-D transformation is similarly given by

$$(t/c)_{T1,2\mathrm{D}} = (t/c)_{T1} \sec \Lambda_{t/c\,\max\,@T1} \tag{12}$$

$$c_{T1,2\mathrm{D}} = c_{T1} \sec \Lambda_{t/c\,\max\,@T1} \tag{13}$$

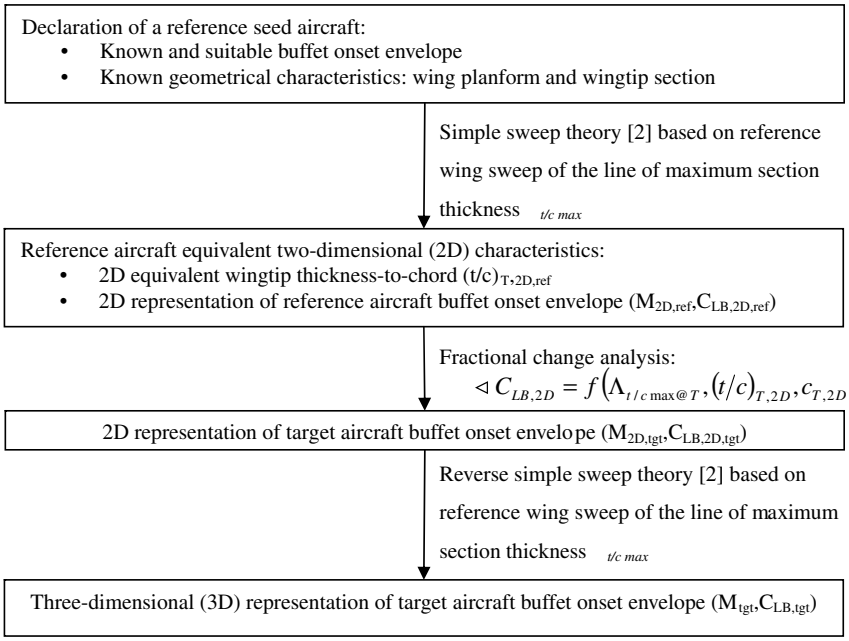

Fig. 5 Flowchart of the proposed semi-empirical buffet onset prediction method.

In the case of the example, the first step is to quantify the seed $L_{t/c\max@T0}$ and target $L_{t/c\max@T1}$ values. Using Eq. (1),

$$\Lambda_{t/c\max@T0} = \tan^{-1}\left[\tan 33.1\,\text{deg} + \left(\frac{4}{6.81}\right)\frac{(0.328-1)}{(0.328+1)}(0.370-0.250)\right]$$

$$\therefore\ \Lambda_{t/c\max@T0} = 31.6\,\text{deg}$$

$$\Lambda_{t/c\max@T1} = \tan^{-1}\left[\tan 27.0\,\text{deg} + \left(\frac{4}{9.00}\right)\frac{(0.250-1)}{(0.250+1)}(0.400-0.250)\right]$$

$$\therefore\ \Lambda_{t/c\max@T1} = 25.2\,\text{deg}$$

Table 3 presents the transformed seed and target aircraft wing section data using Eqs. (10–13). The original seed aircraft 1.0 *g* buffet onset curve and the transformed 2-D version are shown in Fig. 6.

Table 1 ESDU reference parameters for target aircraft wing

Parameter	Value
Λ_{qchd1}, deg	27.0
$(t/c)_{T1}$	0.130
c_{T1}	0.0150
$X_{t/c\max@T1}$	0.400
AR_1	9.00
λ_1	0.250

Table 2 ESDU reference parameters for a seed aircraft wing

Parameter[a]	Value
Λ_{qchd0}, deg	33.1
$(t/c)_{T0}$	0.105
c_{T0}	0.0110
$X_{t/c\max@T0}$	0.370
AR_0	6.81
λ_0	0.328

[a]Note that the wing section parameters are taken at the wingtip airfoil.

2. Consolidated Fractional Change Algorithm

The semi-empirical construct for a 2-D buffet onset definition [i.e., function $C_{LB,2D}$ $(M_{B,2D})$] is based upon the product of the mutually exclusive sensitivity models given by Eqs. (2–6) and the incorporation of $\Theta(M_{B,2D})$, a generic reference curve that is only dependent upon M and is disassociated from the wing geometrical attributes:

$$C_{LB,2D} = [1+\tau\Lambda_{t/c\max@T}]^{\alpha}[1+\omega(t/c)_{T,2D}]^{\beta} \times [1+\vartheta c_{T,2D}]^{\gamma}\Theta(M_{B,2D}) \tag{14}$$

Function $\Theta(M_{B,2D})$ corresponds to the buffet onset of an unswept flat plate with $\lambda = 1.0$ and is a reference that is unique whatever the geometrical configuration of the target wing. The explicit coefficients τ, α, ω, β, ϑ, and γ as well as the implicit coefficients k_1 through k_6 found in Eqs. (3) and (5) are those that need to be determined to establish functional sensitivity between the current wing geometry and the transformed 2-D onset boundary $C_{LB,2D}$.

Transformation of Eq. (14) into a fractional change operator produces

$$C_{LB1,2D}|_{M_{B1,2D}} = C_{LB0,2D}|_{M_{B0,2D}}(1+\triangleleft C_{LB,2D}) \tag{15}$$

To reiterate, it should be noted that the $M_{B,2D}$ array remains constant for the $C_{LB,2D}$ result produced by Eq. (14). As a consequence, this condition infers that the function $\Theta(M_{B,2D})$ remains unchanged as well, which in turn establishes independence from any fractional change transformation. Proceeding with the overall functional transformation, $\triangleleft C_{LB,2D}$ in Eq. (15) can be initially expanded and subsequently factorized to read as

Table 3 Transformed geometric parameters for seed and target aircraft wing sections

Parameter	Value
Seed aircraft	
$(t/c)_{T0,2D}$	0.1233
$c_{T0,2D}$	0.01292
Target aircraft	
$(t/c)_{T1,2D}$	0.1436
$c_{T1,2D}$	0.01658

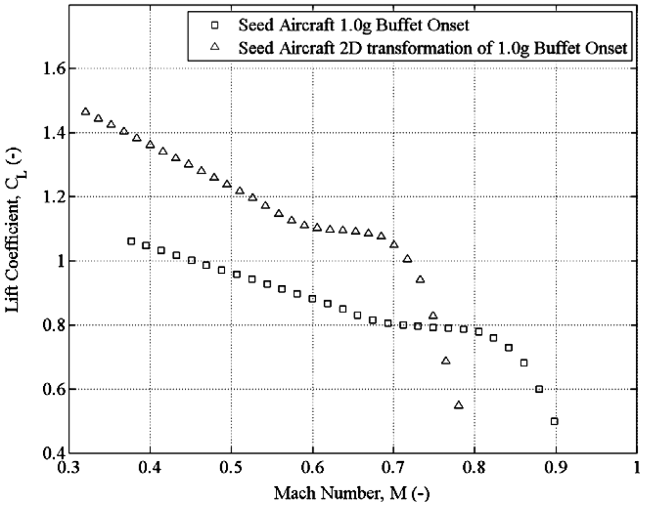

Fig. 6 Original buffet boundary of the example seed aircraft together with its transformed two-dimensional representation (indicative of typical en route center-of-gravity locales).

$$\triangleleft C_{LB,2D} = \frac{C_{LB1,2D} - C_{LB0,2D}}{C_{LB0,2D}} = \frac{C_{LB1,2D}}{C_{LB0,2D}} - 1 \equiv \Phi_{\Lambda_{t/c\max}} \Phi_{(t/c)} \Phi_c - 1 \tag{16}$$

where

$$\Phi_{\Lambda_{t/c\max}}|_{M_{B,2D}} = \left[1 + \frac{\tau \Lambda_{t/c\max @T0}}{\tau \Lambda_{t/c\max @T0} + 1} \triangleleft \Lambda_{t/c\max @T}\right]^{\alpha} \quad \forall\ \Lambda_{t/c\max @T0} \neq 0 \tag{17a}$$

$$\Phi_{(t/c)}|_{M_{B,2D}} = \left[1 + \frac{\omega (t/c)_{T0,2D}}{\omega (t/c)_{T0,2D} + 1} \triangleleft (t/c)_{T,2D}\right]^{\beta} \quad \forall\ (t/c)_{T0,2D} > 0 \tag{17b}$$

$$\Phi_c|_{M_{B,2D}} = \left(1 + \frac{\vartheta c_{T0,2D}}{\vartheta c_{T0,2D} + 1} \triangleleft c_{T,2D}\right)^{\gamma} \quad \forall\ c_{T,0,2D} \neq 0 \tag{17c}$$

where the angles $\Lambda_{t/c\max @T}$ are expressed in degrees.

Thus, upon substitution of Eq. (16) into Eq. (15), the final functionally transformed 2-D buffet onset model becomes

$$C_{LB1,2D}|_{M_{B1,2D}} = C_{LB0,2D}|_{M_{B0,2D}} \Phi_{\Lambda_{t/c\max}} \Phi_{(t/c)} \Phi_c \tag{18}$$

with the corresponding condition of

$$M_{B1,2D} = M_{B0,2D} \tag{19}$$

The fortuitous consequence of Eq. (18) is that if the explicit coefficients (τ, α, ω, β, ϑ, and γ) and the implicit coefficients (k_1 through k_6) are derived via nonlinear data regression techniques, the designer/analyst will gain a well-rounded understanding of the independent parameters' functional sensitivities, because absolute and relative differences can be inspected directly. This possibility fulfills the modeling tenet of transparency discussed in Sec. II, "Buffet Prediction Algorithm Synthesis." In addition, due to the relative nature of the sensitivity construct offered by Eq. (18), this beneficially permits the use of any reference buffet onset curve, whether it is a user-specified reference aircraft wing or a generic reference wing that is ubiquitously applicable. The modeling tenet of conformity in relation to applicability for predictions outside the bounds of an original training data set is therefore satisfied. The very nature of the $C_{LB,2D}$ prediction scheme given by Eq. (18) also fulfills the remaining modeling tenets of consistency (physical significance), scope (covers explicit and implicit functional sensitivity), and malleability (alterations to the functional sensitivity operators of one or more design variables can be incorporated without the need to distort the unaltered constituents).

Although the method given previously fulfills the five tenets thus far considered out of the six required for declaration of a useful and flexible mathematical model, the reader is warned of one pertinent limitation. The fractional change operators $\Phi_{\Lambda t/c\max}$, $\Phi_{t/c}$, and Φ_c given by Eq. (17) will not permit functional sensitivity with $C_{LB,2D}$ if the seed condition is defined as $\Lambda_{t/c\max @T0} = 0$ deg and/or $(t/c)_{T0,2D} = 0$ and/or $c_{T0,2D} = 0$. In other words, due to declaration of a null seed condition, it is analytically impermissible to predict $C_{LB1,2D}$ for any nonzero variation to target $\Lambda_{t/c\max @T1}$ and/or $(t/c)_{T1,2D}$ and/or $c_{T1,2D}$. Apart from the fact that $(t/c)_{T0,2D} \leq 0$ lacks any physical meaning, the authors concede that the special condition for $L_{t/c\max @T0}$ and $c_{T0,2D}$ does compromise the desire to declare model consistency without caveats. With regard to wing section c, prediction based upon variations away from a symmetrical section seed will not be allowed; however, the method does afford transformation of a seed wing section with nonzero c into a symmetric section (i.e., $c_{T1,2D} = 0$). To sum up, the designer/analyst is therefore advised to check and, when required, subsequently adopt a seed aircraft and associated wing geometry that does not violate the previously mentioned constraints. Notwithstanding these special conditions, as will be shown hereafter, the mathematical construct given by Eq. (17) that attempts to establish functional sensitivity of $\Lambda_{t/c\max}$ and c to C_{LB} does prove to be satisfactory when it concerns the modeling tenet of conformity within the bounds of the original data set.

As an exemplar of how the fractional change operation is computed, the design parameter $\Lambda_{t/c\max @T}$ will be reviewed here for the example aircraft. The fractional change in $\Lambda_{t/c\max @T}$ or $\triangleleft \Lambda_{t/c\max @T}$ is found via use of Eq. (7): namely,

$$\triangleleft \Lambda_{t/c\max @T} = \frac{\Lambda_{t/c\max @T1}}{\Lambda_{t/c\max @T0}} - 1 \quad \therefore\ \triangleleft \Lambda_{t/c\max @T} = -0.2025$$

Because the function $\Phi_{\Lambda t/c\max @T}$ given by Eq. (17a) contains the explicit coefficient $\alpha = f(M_{2D})$ as defined by Eq. (3), $\Phi_{\Lambda t/c\max}$ will need to be computed for each value of M_{2D} offered in the seed aircraft buffet onset data set. Similarly, the function $\Phi_{(t/c)}$ needs to be calculated using Eq. (17b), with corresponding explicit coefficient $\omega = f(M_{2D})$ defined by Eq. (5). The fractional change in $(t/c)_{T,2D}$ or $\triangleleft (t/c)_{T,2D}$ is

$$\triangleleft (t/c)_{T,2D} = \frac{(t/c)_{T1,2D}}{(t/c)_{T0,2D}} - 1 \quad \therefore\ \triangleleft (t/c)_{T,2D} = +0.1646$$

Similarly, the fractional change in $c_{T,2D}$ or $\triangleleft c_{T,2D}$ is

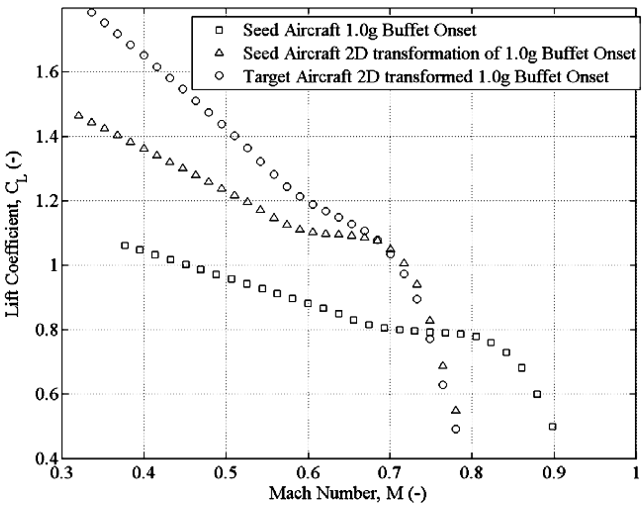

Fig. 7 Transformed two-dimensional buffet onset of the target aircraft obtained by fractional change from the seed aircraft (indicative of typical en route center-of-gravity locales).

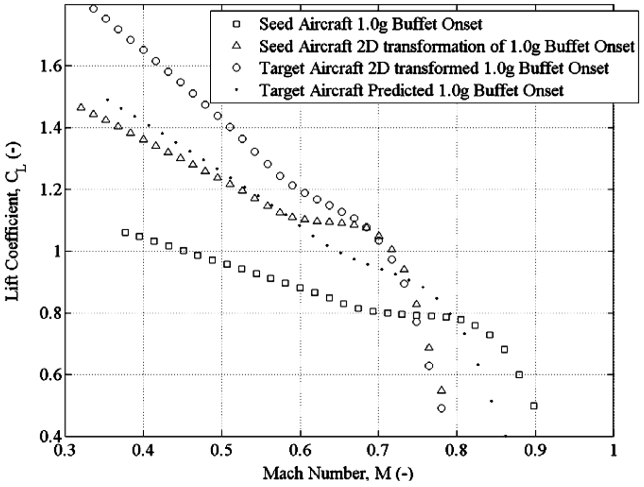

Fig. 8 Final predicted 1.0 *g* buffet onset of the target aircraft obtained by fractional change from the seed aircraft (indicative of typical en route center-of-gravity locales).

$$\triangleleft c_{T,2D} = \frac{c_{T1,2D}}{c_{T0,2D}} - 1 \quad \therefore \triangleleft c_{T,2D} = +0.2833$$

Knowing the explicit coefficients ($\tau, \alpha, \omega, \beta, \vartheta$ and γ) and the implicit coefficients (k_1 through k_6) (which will be given explicitly in Sec. III, "Presentation of a Practical Buffet Onset Prediction Tool," and Sec. III.B, "Final Buffet Onset Model Selection and Discussion"), completion of the entire array of fractional change operations generates the 2-D buffet onset of the new aircraft, as shown in Fig. 7.

3. Three-Dimensional Transformation

Once account is made of the target wing geometry influence on the 2-D buffet onset, the prediction process is completed by application of simple sweep theory: namely,

$$M_{B1} = M_{B1,2D} \sec \Lambda_{t/c\,\max\,@T1} \tag{20}$$

$$C_{LB1} = C_{LB1,2D} \cos^2 \Lambda_{t/c\,\max\,@T1} \tag{21}$$

In the case of the example aircraft, the final result is shown in Fig. 8, together with a contrast against the original seed aircraft 1.0 *g* buffet onset, transformed 2-D buffet onset curve for the seed aircraft, and the target aircraft 2-D transformed locus.

III. Presentation of a Practical Buffet Onset Prediction Tool

Nonlinear data regression analysis was performed on the model given by Eq. (14) using a training data set comprising 15 in/out-of-production and in/out-of-service civil transport aircraft. Table 4 presents the aircraft designation, classification, typical operating cruise regime, powerplant type, and morphological attributes.

The data set of aircraft spans a measure of scale [i.e., supermidsize to ultra-long-range executive (business) aircraft and medium-size regionals to very large long-range wide bodies]; distinct mission roles (i.e., business aircraft versus airliners); distinct morphological attributes [i.e., on-wing, underwing podded, and aft-fuselage-mounted propulsion, with winglets (or wingtip fences) and without]; distinct propulsion type (i.e., high-speed turboprop versus turbofan); and a measure of maximum speed capability (i.e., high subsonic to high transonic).

Before presenting the derived coefficients of proportionality, an important assumption incorporated into the work needs to be discussed. As mentioned previously, the critical wing section location and corresponding geometric attributes are typically based on 70–80% wing semispan because, in practice, it is the traditional critical design case (in which the separation occurs first). The final buffet onset model ended up using the wingtip section parameters $\Lambda_{t/c\,\max\,@T}$, $(t/c)_T$, and c_T, because investigation of a number of wing thickness distributions showed that the wing section critical to buffet onset and the wingtip section geometric characteristics can be suitably correlated with one another. A further argument for favoring the wingtip section is the fact that it is simply convenient to use. Indeed, topological descriptions along the wingspan are not usually known at the conceptual design stage, whereas the root and tip sections are usually known. The root wing section is disregarded for buffet onset prediction because the critical (actual design) section is located closer to the wingtip.

A. Reference Wing Convention

The equivalent reference wing is a representation of an actual cranked (discontinuity in the leading and/or trailing edge) wing by a fictitious simplified planform that extends toward the aircraft centerline. For the sake of reducing the array of primary design parameters that need to be considered for sizing and optimization, the overall geometric characteristics of an actual wing with cranks or notches in the planform geometry are replaced by a suitable representative: namely, an equivalent straight trapezoid. A number of reference wing conventions are currently used by industry and academia [7], and as a result, basic design parameter quantities for S_W, L_{Qchd}, aspect ratio, and λ will all be distinct between each of these definitions.

Table 4 Details about transport aircraft data set used for nonlinear regression analysis

Designation	Classification	Typical cruise regime	Powerplant number, type, and locale[a]	Morphological attributes
Airbus 320-100	Large narrow body	Midtransonic	2 × TFWP	Low wing, single crank, medium sweep, wingtip fence
Airbus A330-200	Wide body	High transonic	2 × TFWP	Low wing, single crank, high sweep, wingtip fence
Boeing B737-800	Large narrow body	Midtransonic	2 × TFWP	Low wing, single crank, medium sweep, no winglets
Boeing B747-100	Very large wide body	High transonic	4 × TFWP	Low wing, multiple crank, high sweep, no winglets
Boeing B757-200	Large narrow body	Midtransonic	2 × TFWP	Low wing, single crank, medium sweep, no winglets
Boeing DC10-10	Wide body	High transonic	2 × TFWP 1 × TFAF	Low wing, single crank, high sweep, no winglets
Boeing MD-80	Medium narrow body	Midtransonic	2 × TFAF	Low wing, multiple crank, medium sweep, no winglets
Bombardier Challenger 300	Supermidsize executive	Midtransonic	2 × TFAF	Low wing, single crank, medium sweep, winglets
Bombardier Challenger CL-604	Large executive	Midtransonic	2 × TFAF	Low wing, multiple crank, medium sweep, winglets
Bombardier CRJ-200	Medium regional	Midtransonic	2 × TFAF	Low wing, multiple crank, medium sweep, winglets
Bombardier CRJ-700/900	Large regional	Midtransonic	2 × TFAF	Low wing, single crank, medium sweep, winglets
Bombardier Global Express	Ultra long-range executive	High transonic	2 × TFAF	Low wing, multiple crank, high sweep, winglets
Fokker F-100	Small narrow body	Low transonic	2 × TFAF	Low wing, single crank, low sweep, no winglets
McDonnell Douglas DC8	Medium-to-large narrow body	Midtransonic	4 × TFWP	Low wing, single crank, medium sweep, no winglets
Saabaerosystems Saab 2000	Medium regional	High subsonic	2 × TPW	Low wing, no crank, low sweep, no winglets

[a]TFWP denotes the turbofan wing podded, TFAF denotes the turbofan aft fuselage, and TPW denotes the turboprop on wing.

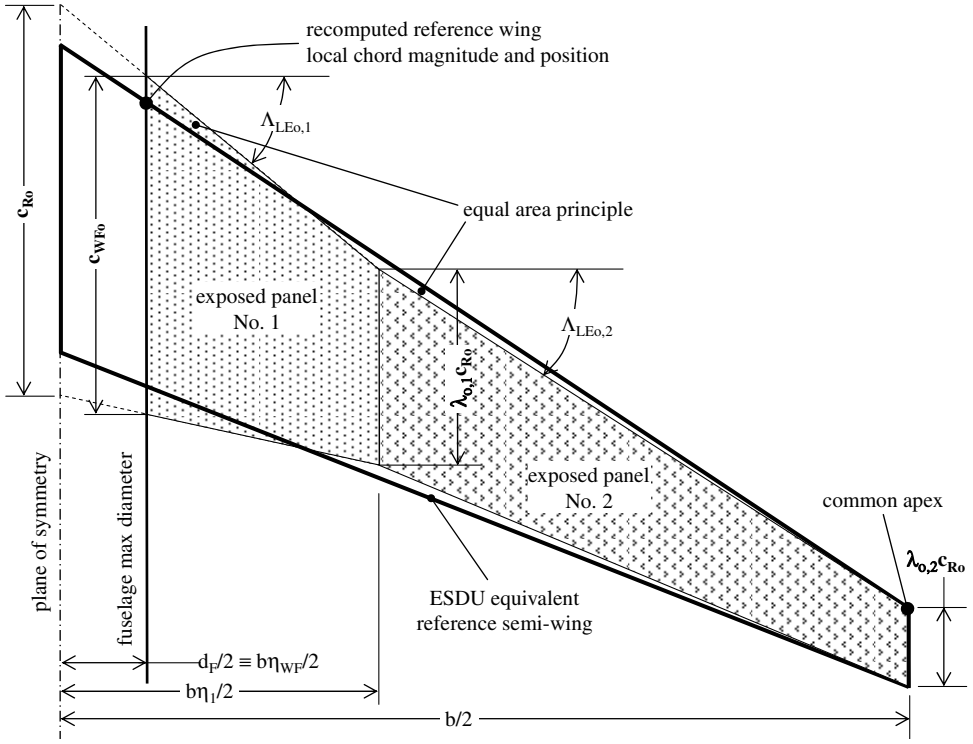

Fig. 9 Equivalent reference wing geometric definition using the ESDU method; in this presentation, maximum fuselage diameter locale is assumed to be a suitable proxy for wing–fuselage juncture.

1. ESDU Reference Wing

The concept of the ESDU equivalent wing planform [8] (as shown in Fig. 9) was first published in 1976. Since that time, it has been employed with a growing popularity and has become a standard in numerous academic institutions and airframe manufacturers.

Fundamentally, to define the ESDU reference wing (as shown in Fig. 9), the designer/analyst needs to take account of the following geometric parameter values: the wing span excluding wingtip devices b; nondimensional wing–fuselage juncture spanwise locale parameter η_{WF}; number of panels N; nondimensional spanwise locale at the termination of each trapezoidal panel (η_n, where n denotes the trapezoid panel number); gross wing root chord c_{Ro}; gross wing taper ratio(s) $\lambda_{o,n}$, where n denotes trapezoidal panel number, with each referred to c_{Ro}; and the gross wing leading-edge sweep(s) $\Lambda_{\mathrm{LE}o,n}$, where n denotes the trapezoid panel number.

2. Transforming from ESDU to an Alternate Reference Wing Convention

Aircraft integrators are usually inclined to adopting unique in-house-developed technical methodologies and conventions for purposes of tailoring specifically to their respective design philosophies. Accordingly, there exist other reference wing definitions, and two notable examples are the Airbus Gross [7,9] and Boeing Wimpress [7,10] methods. Details regarding the analytical process in defining an Airbus Gross or Boeing Wimpress reference wing will not be discussed here; the reader is advised to access relevant material given in [7,9,10] for further elaboration.

In view of the presented buffet onset prediction algorithm conforming to the ESDU reference wing standard, the correlation coefficients found in Eq. (14) are not, in principle, consistently applicable for alternate reference wing conventions. To this end, the authors recommend performing a geometric transformation such that the results produced by the method presented in this paper can be augmented to conform to any desired reference wing convention. To continue, a transformation of the predicted buffet onset from the ESDU standard ($C_{LB,\mathrm{ESDU}}$) to an alternate reference wing convention ($C_{LB,\mathrm{AREF}}$) is performed using the basic identity

$$C_{LB,\mathrm{AREF}} = \frac{S_{W,\mathrm{ESDU}}}{S_{W,\mathrm{AREF}}} C_{LB,\mathrm{ESDU}} \tag{22}$$

where $S_{W,\mathrm{ESDU}}$ represents the ESDU reference wing area, and $S_{W,\mathrm{AREF}}$ is the reference wing area of an alternate convention. Using the geometric definitions given in Fig. 9, $S_{W,\mathrm{ESDU}}$ can be quantified using the relation

$$S_{W,\mathrm{ESDU}} = \frac{S_{\mathrm{exp}} - b\lambda_{o,N}c_{Ro}\eta_{\mathrm{WF}}(1-\eta_{\mathrm{WF}})}{(1-\eta_{\mathrm{WF}})^2} \tag{23}$$

where $\lambda_{0,N}$ represents the taper ratio of the wingtip, and the exposed wing planform area S_{exp} is computed using Eq. (24), given next:

$$S_{\mathrm{exp}} = \frac{b}{2}c_{Ro}\left\{\left(\frac{\eta_{\mathrm{WF}}}{\eta_1}\right)(\eta_1-\eta_{\mathrm{WF}})\left[\frac{1+\lambda_{o,1}}{\eta_{\mathrm{WF}}/\eta_1}+\lambda_{o,1}-1\right] + \sum_{n=2}^{N}(\eta_n-\eta_{n-1})(\lambda_{o,n-1}+\lambda_{o,n})\right\} \tag{24}$$

Although transformation of $C_{LB,\mathrm{ESDU}}$ has been given by Eqs. (22–24), it is highlighted that the buffet onset prediction yielded by Eq. (14) stipulates reference wing convention compatibility between the correlation coefficients and declaration of design parameters

Table 5 Identification of the best buffet onset models with regard to conformity

Clustered data set of aircraft	Number of aircraft in data set	Average error in predicted C_{LB}	Standard error in predicted C_{LB}
With winglets	7	0.000361	0.0217
Without winglets	8	−0.00360	0.0255
Aft-fuselage-mounted propulsion	7	0.000339	0.0239
Underwing podded propulsion	8	−0.00370	0.0257
All aircraft in data set	15	0.000791	0.0262

Table 6 Recommended regression coefficients for predicting buffet onset (conforms to ESDU convention)

Explicit coefficients	Implicit coefficients	Coefficient value	Reference equation
τ	N/A	10.000	(19)
α	k_1	−0.1024	(6)
α	k_2	1.0000	(6)
α	k_3	2.4872	(6)
ω	k_4	0.2963	(8)
ω	k_5	−1.0000	(8)
ω	k_6	3.1464	(8)
β	N/A	25.353	(19)
ϑ	N/A	2.0364	(19)
γ	N/A	10.050	(19)

values for the explicit set $\Lambda_{t/c\,\max}$, t/c, and c and the implicit set Λ_{qchd}, aspect ratio, and λ found in Eq. (1). It is therefore incumbent upon the designer/analyst to treat the aircraft design candidate according to procedures dictated by the ESDU convention provided in [8].

B. Final Buffet Onset Model Selection and Discussion

In an effort to identify the best conforming model(s), nonlinear regression analysis was performed on various versions of the original 15-aircraft data set. The all-aircraft ESDU reference wing conforming data set comprised 1.0 g buffet onset information based upon typical en route center-of-gravity locales and was bounded according to the following: $\Lambda_{\text{qchd,dats}} \in [3.60\,\text{deg}, 35.6\,\text{deg}]$; $(t/c)_{T,\text{dats}} \in [0.0868, 0.120]$; $c_{T,\text{dats}} \in [0.0100, 0.0166]$; $X_{t/c\,\max\,@T,\text{dats}} \in [0.320, 0.474]$; $\text{AR}_{\text{dats}} \in [6.81, 11.0]$; and $\lambda_{\text{dats}} \in [0.190, 0.375]$. Table 5 presents an array of modeling suitability metrics (namely, average error and the standard error of estimate ε_{SEE}),

$$\varepsilon_{\text{SEE}} = \sqrt{\frac{\sum (z_{\text{est}} - z_{\text{act}})^2}{n}} \tag{25}$$

to ascertain the level of conformity achieved when clustering the data set into specific aircraft morphological categories. The examined categories included those with winglets or wingtip fences, without winglets or wingtip fences, aft-fuselage-mounted propulsion, underwing podded propulsion, and the complete original 15-aircraft data set.

Review of Table 5 indicates that the clustered data set of aircraft without winglets and the clustered data set of aircraft with underwing podded propulsion system, notwithstanding a reasonable SEE value, produced a high magnitude of average error result. Acceptable levels of magnitude of average error were produced by data sets comprising aircraft with winglets, aft-fuselage-mounted propulsion systems, and the all-aircraft cluster. In view of the fact that the act of clustering for unique coefficients of proportionality did not generate an approximately homogenous distribution and consistently lower values of SEE and magnitude of average error, the adoption of the all-aircraft data set that encompasses different vehicular morphologies was deemed to be the least complex method for predicting the 1.0 g buffet onset envelope. This analysis exemplifies adherence to the tenets of conformity and robustness in relation to creation of suitable mathematical models for purposes of conceptual design prediction.

Based upon the aforementioned reasoning, the final set of coefficients conforming to an ESDU reference wing convention recommended for the prediction of transport aircraft buffet onset boundary is given in Table 6. Normally, a seed aircraft 1.0 g buffet onset envelope is used in conjunction with the regression coefficient values shown in Table 6. For those occasions in which a seed aircraft buffet onset envelope is not available, a generic functional description of the generic $C_{LB,\text{2D}}$ and C_{LB} derived during the nonlinear regression exercise based upon the original 15-aircraft data set discussed previously can be used and is presented in Table 7 and Fig. 10, respectively. This generic 1.0 g buffet onset locus is akin to capturing a ubiquitous snapshot of the technology level employed on modern transport aircraft. Although the 3-D 1.0 g buffet onset locus given in Table 7 is described only up to $M_{B,\text{gen}} = 0.830$, invoking simple sweep theory to facilitate transformation to a physically relevant plane enables the ability to describe a 3-D buffet envelope for any target aircraft up to and beyond its intended M_{MO} speed.

The corresponding ESDU reference wing geometry parameters can be found in Table 8, and a visual representation of the straight trapezoid is presented in Fig. 11. Curiously, it can be observed that the generic reference wing is representative of a medium-size regional turbofan aircraft or supermidsize to large executive turbofan aircraft. As a check that the nonlinear regression exercise demonstrates an implicit measure of conformity, it was confirmed that the generic reference wing parameters presented in Table 8 fall within the bounded values of the original 15-aircraft data set from whence it originated.

Applying the tests for physical significance discussed earlier, the implicit coefficients k_1 through k_3 that collectively define the explicit α coefficient given in Eq. (3) and k_4 through k_6 that collectively define the explicit ω coefficient given in Eq. (5) were investigated to ascertain algorithmic consistency. Examining the case for the α coefficient (i.e., solving for $M_{B,\text{2D}}$ at condition $\alpha = 0$), the result was calculated to be $M_{B,\text{2D}} = 0.400$, which corresponds to a 3-D Mach $M_B = 0.439$ for the generic reference wing. This correlates well against the physically tangible threshold between buffet due to subsonic leading-edge separation and low-transonic mixed separation as espoused by Mabey [5]. In addition, upon examination of the case for the ω coefficient (i.e., solving for $M_{B,\text{2D}}$ at condition $\omega = 0$), the result was calculated to be $M_{B,\text{2D}} = 0.679$, which corresponds to a 3-D Mach $M_B = 0.746$ for the generic reference wing. Again, this correlates well against the physically tangible threshold between buffet induced by low-transonic mixed separation and midtransonic strong shock formation as presented by Mabey [5]. Based upon the analytical solutions given previously, the three zones of 1.0 g buffet onset illustrated in Fig. 3 earlier

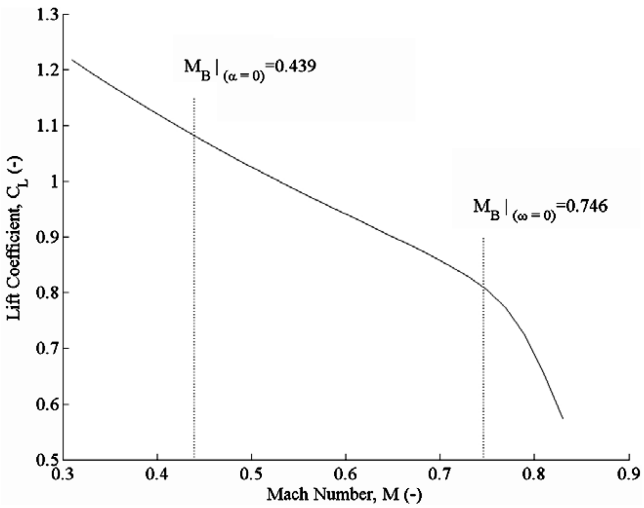

Fig. 10 Generic three-dimensional 1.0 g buffet onset derived from regression analysis performed on the 15-aircraft data set (indicative of typical en route center-of-gravity locales).

Table 7 Generic three-dimensional 1.0 *g* buffet-envelope data (conforms to ESDU convention)[a]

$M_{B,\text{gen}}$	0.3100	0.3300	0.3500	0.3700	0.3900	0.4100	0.4300	0.4500	0.4700
$C_{LB,\text{gen}}$	1.2178	1.1953	1.1733	1.1520	1.1313	1.1112	1.0912	1.0717	1.0529
$M_{B,\text{gen}}$	0.4900	0.5100	0.5300	0.5500	0.5700	0.5900	0.6100	0.6300	0.6500
$C_{LB,\text{gen}}$	1.0346	1.0166	0.9993	0.9826	0.9664	0.9501	0.9333	0.9160	0.8997
$M_{B,\text{gen}}$	0.6700	0.6900	0.7100	0.7300	0.7500	0.7700	0.7900	0.8100	0.8300
$C_{LB,\text{gen}}$	0.8841	0.8671	0.8486	0.8287	0.8050	0.7722	0.7224	0.6541	0.5750

[a]Indicative of typical en route center-of-gravity locales.

Table 8 ESDU reference geometric parameters for a derived generic wing

Parameter	Value
$\Lambda_{\text{qchd,gen}}$, deg	26.14
$\Lambda_{t/c\,\text{max,gen}}$, deg	24.42
$(t/c)_{T,\text{gen}}$	0.1101
$c_{T,\text{gen}}$	0.0115
$X_{t/c\,\text{max}\,@T,\text{gen}}$	0.3763
AR_{gen}	7.889
λ_{gen}	0.2698

(including the Mach number thresholds that delineate subsonic buffet due to leading-edge separation, buffet due to mixed separation, and transonic shock-induced buffet) are suitably represented. This satisfies the edict of consistency for the proposed buffet onset model.

Starting from the generic reference locus described in Table 7 and corresponding generic reference wing given in Table 8 and applying the method described in Eqs. (8–21), the 1.0 *g* buffet onset was predicted for the same aircraft that supported the original data set from which the coefficients in Table 6 were derived. The residuals result shown in Fig. 12 display for each aircraft the relative and absolute errors in lift coefficient for 1.0 *g* buffet onset over a range of Mach numbesr that cover typical initial climb, en route climb, descent, and cruise speeds up to M_{MO}.

Figure 12 demonstrates that for any aircraft in any en route flight phase (speeds at which $M \geq 0.400$), the maximum absolute error bandwidth is $-0.0773 \leq \varepsilon \leq +0.0644$. In terms of relative error, the maximum bandwidth was found to be $-8.51\% \leq \varepsilon \leq +8.98\%$. Notwithstanding these observed extremes in error, it can be stated that most predictions for 1.0 *g* buffet onset clearly fall within a relative error of $\pm 5.0\%$, with occasional excursions for some aircraft toward the higher-speed regime (i.e., lower attainable lift coefficients). These excursions can be characterized as falling well within a relative error of $\pm 9.0\%$. This result is considered to be satisfactory in relation to expected performance for purposes of conceptual design prediction. Taking stock of $\text{SEE} = 0.0262$ presented earlier, this reinforces the validity of the various theoretical assumptions made for the proposed 1.0 *g* buffet onset prediction methodology.

Considering again the example given in Sec. II, "Buffet Prediction Algorithm Synthesis" and Sec. II.D, "Semi-Empirical Buffet Onset Model Construct," the buffet onset of the example target aircraft has been recomputed using the generic 1.0 *g* buffet onset curve and generic reference wing geometric data given in Tables 7 and 8 as seed aircraft. The results are presented in Fig. 13, which compares and contrasts the predicted 1.0 *g* buffet envelopes of the target aircraft design candidate obtained by the two methods (i.e., using a known aircraft or using the provided generic aircraft as seeds). It can be observed that the two methods give very similar results when it concerns the values of C_{LB} for a given Mach number, with one exception: there are some discrepancies in the geometrical progression and shape of the curves, particularly in the low-transonic-speed regime. The discrepancy within the low-transonic regime is attributable to the known aircraft seed having pronounced mixed-flow-separation (due to transonic reattachment) physical characteristics and thus reinforces the notion that the onus is on the designer/analyst to choose a suitable seed aircraft if higher levels of numerical and physical conformity are desired. The difference in prediction between selecting a known aircraft and a generic aircraft as seed was found to be with a $\pm 5.0\%$ bandwidth for the range $0.40 \leq M \leq M_{\text{MO}}$, which encompasses any normal and abnormal en route flight operations. This observation demonstrates that use of the provided generic aircraft reference geometry and associated buffet onset curve generates satisfactory results with regard to the predicted values and range of the buffet onset and provides an adequate description of the global progression.

Finally, as a contrast between the 1.0 *g* buffet onset prediction method expounded in this paper and those methods employed in contemporary industrial conceptual design analysis, Fig. 13 also contains plots showing predicted buffet envelopes using methods espoused by [1,3]. It is evident that the industrial conceptual design prediction methods exhibit poor levels of conformity against the proposed method for Mach numbers lower than midtransonic speeds. This is an expected outcome, because the industrial methods only reflect function sensitivity for buffet onset generated by strong-shock-induced separation and so would tend to not capture design parameter influences with regard to pure leading-edge-borne separation at the subsonic speed regime or the phenomena behind mixed-separation at low-transonic speeds.

Finally, as another demonstration of the robustness that the proposed method offers, a study was performed in which one of the aircraft in the data set was declared as a seed and subsequently transformed into a target aircraft (also part of the original data set) with quite different morphological and geometrical attributes compared with the seed. The method was applied to predict the 1.0 *g* buffet onset of the Saab 2000 medium-size regional turboprop (thick, no crank, low-sweep wing, and powerplant integrated on the wing with the undercarriage) assuming the Global Express ultra-long-range executive jet (thin, multiple-crank, high-sweep wing, and powerplant mounted on the aft fuselage) as a seed aircraft. The results are presented in Fig. 14.

Considering a speed range of $0.35 \leq M \leq M_{\text{MO}}$, a maximum relative difference bandwidth of $-8.14\% \leq \varepsilon \leq +4.49\%$ was computed in predicting the Saab 2000 maximum attainable lift coefficient for 1.0 *g* buffet onset. In contrast, if the previously mentioned generic aircraft reference wing and associated buffet onset locus were adopted as seeds, the maximum relative error bandwidth was found to be $-2.15\% \leq \varepsilon \leq 3.89\%$. Irrespective of the significant differences in morphology and geometric attributes between the two aircraft, the method produces prediction results for the Saab 2000 that conforms satisfactorily between typical initial climb speed and M_{MO} thresholds compared with the actual 1.0 *g* buffet envelope. Variations in relative conformity for subsonic-to-

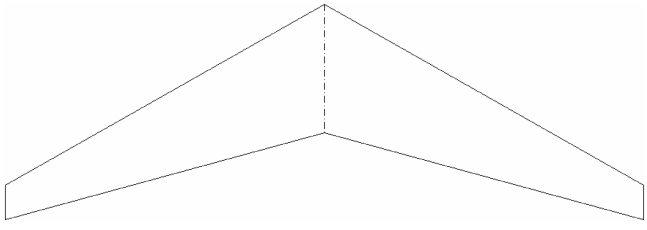

Fig. 11 ESDU reference wing planform for derived generic wing.

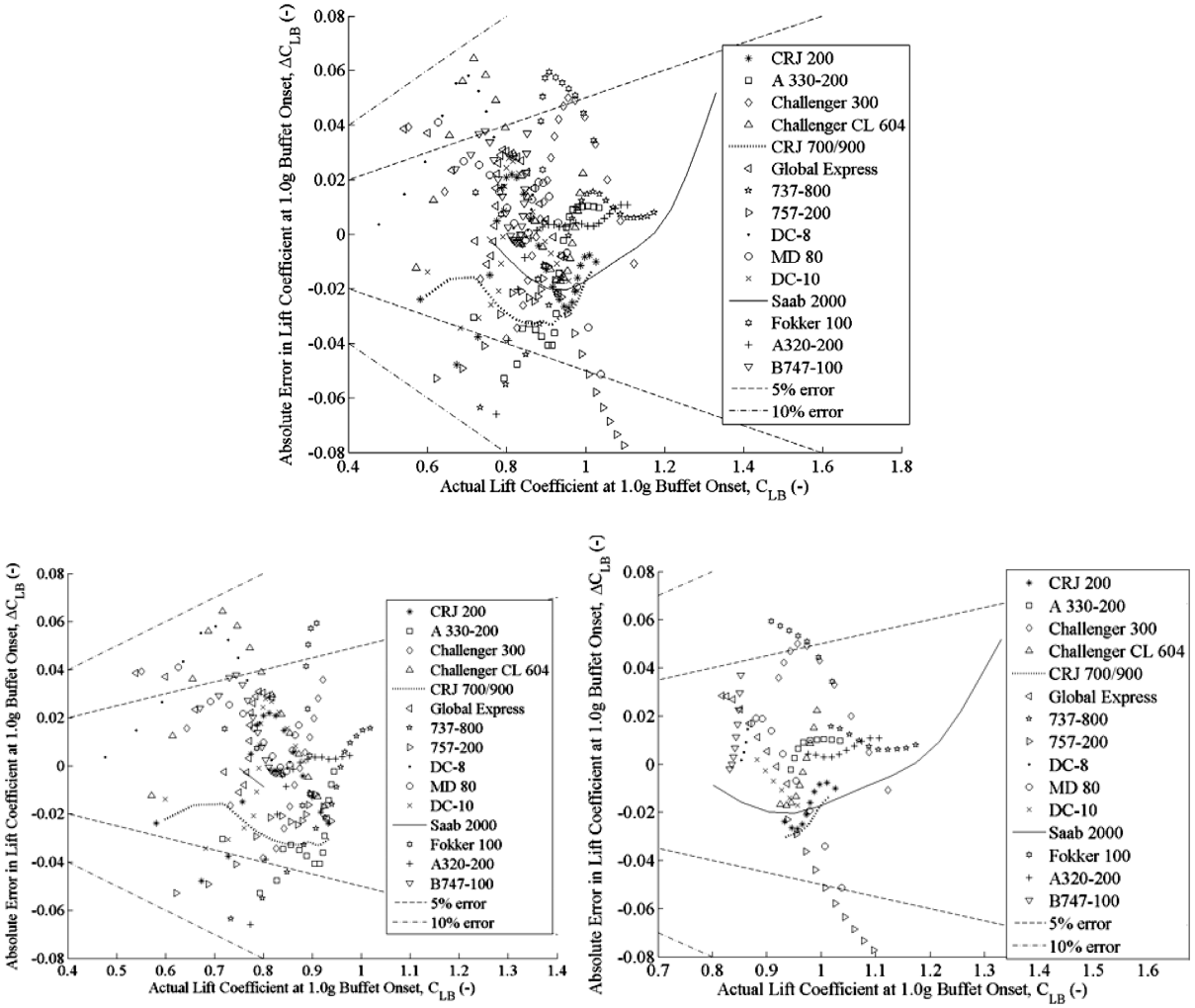

Fig. 12 Error in lift coefficient for 1.0 *g* buffet onset produced using the derived generic reference wing as a seed (indicative of typical en route center-of-gravity locales); all Mach numbers (top), $M \geq 0.60$ (bottom left), and $M < 0.60$ (bottom right).

low-transonic speeds of the Saab 2000 is attributable to the fact that the seed Global Express aircraft buffet boundary has pronounced flow reenergization within the mixed-separation regime, whereas the Saab 2000 transition from leading-edge to weak-shock-induced separation does not benefit from an enhanced level of transonic reattachment. This exemplifies the notion that even though the proposed method for 1.0 *g* buffet onset displays desirable qualities of consistency and robustness, the onus is on the designer/analyst

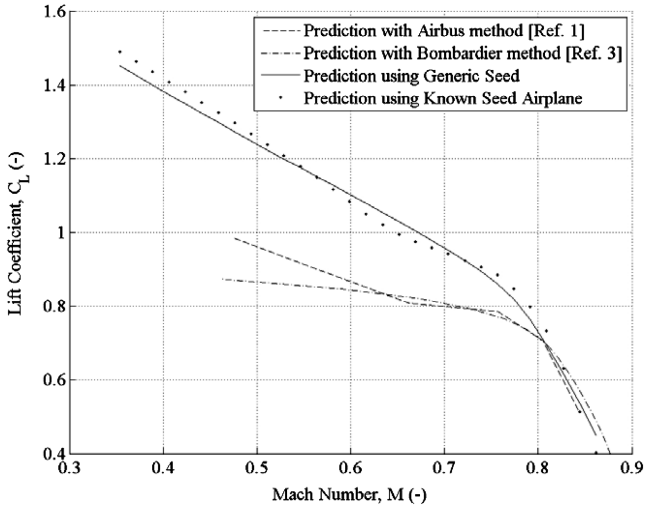

Fig. 13 Comparison of the estimated 1.0 *g* buffet onset of the target geometry using the previously described method starting from a known or from a generic seed and using the Airbus method and Bombardier Aerospace method (indicative of typical en route center-of-gravity locales).

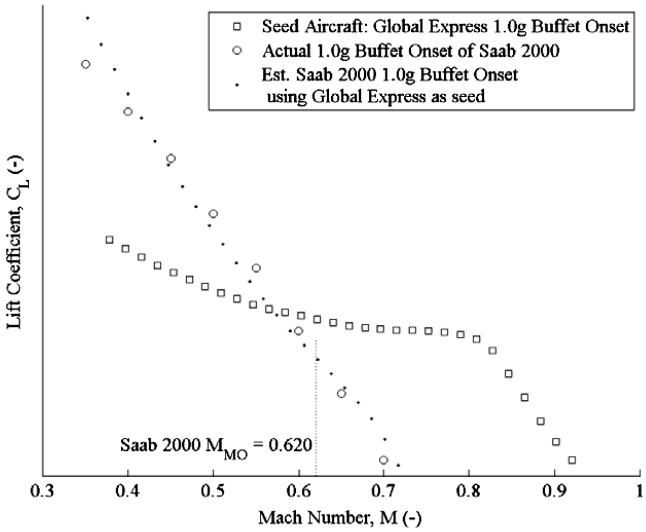

Fig. 14 Example prediction of the Saab 2000 regional turboprop 1.0 *g* buffet onset assuming the Global Express ultra-long-range executive jet as the seed aircraft (indicative of typical en route center-of-gravity locales).

to choose a suitable seed aircraft if higher levels of numerical and physical conformity are desired.

IV. Conclusions

This paper has presented a semi-empirical physically relevant method to predict the buffet onset envelope of transport category aircraft by using an array of commonly used conceptual design variables associated with wing attributes. A total of six wing-related design parameters have been declared to have functional sensitivity with the maximum attainable lift coefficient for buffet onset: reference wing aspect ratio, reference wing taper ratio, reference wing quarter-chord sweep, wingtip section maximum thickness-to-chord ratio, wingtip section maximum thickness chordwise position, and wingtip section maximum camber. The first four parameters are typically manipulated for sizing purposes during the conceptual design stage, and the last two parameters offer potential to extend the scope of design sensitivities to accommodate a more detailed aerodynamic optimization treatment. The mutually exclusive nature of the method's analytical construct provides considerable freedom in deciding the scope of free-design-variable complexity.

Two variants of this method are proposed. The first allows the designer/analyst to use a generic reference curve and associated generic reference wing to evaluate the buffet envelope of the target aircraft geometry. Doing so gives a good description of the global trend of the buffet onset of the target geometry, and the results of validation for several quite different aircraft geometries and morphologies show that it conforms well against their actual buffet data. The second method uses a known seed aircraft instead of starting from the provided generic reference buffet curve. This alternate approach also produces good results and, in addition, enables the designer/analyst to retain the underlying in-house technology and know-how peculiar to an aircraft product or an aircraft integrator's design philosophy that are implicitly revealed by the seed airplane details of the buffet-envelope geometrical progression. Therefore, when possible, it is advised that this second variant of the method should be used.

Regarding relative error ε in maximum attainable lift coefficient prediction when using the derived correlation coefficient values from nonlinear regression analysis, the maximum absolute error bandwidth was found to be $-0.0773 \leq \varepsilon \leq +0.0644$ or, equivalently, the maximum relative error bandwidth was found to be $-8.51\% \leq \varepsilon \leq +8.98\%$. Notwithstanding these observed extremes in error, it was shown that most predictions for buffet onset clearly fell within a relative error of $\pm 5.0\%$, with occasional excursions characterized as falling well within a relative error of $\pm 9.0\%$. Together with a computed standard error of estimate value of 0.0262, the prediction method for lift coefficient at buffet onset for a given Mach number was considered to be satisfactory when benchmarked against expected performance for purposes of conceptual design sizing. In closing, the method presented here appears to be relatively simple, economical, flexible, and sufficiently robust for application to most geometrical and morphological variations employed for contemporary transport category aircraft.

References

[1] Anon., *Airbus UK Design Manual for the University of Bristol 2007/2008 Undergraduate Aircraft Design Project*, Univ. of Bristol, Bristol, England, U.K., 2007, Sec. 7.

[2] Jones, R. T., "Wing Plan Forms for High-Speed Flight," NACA TN 1033, 1946.

[3] Pepin, F., "Empirical Formulas for the Prediction of Buffet Onset," Bombardier Aerospace, Montreal, Quebec, Canada, 2002.

[4] Isikveren, A., "Parametric Modeling Techniques in Industrial Conceptual Transport Aircraft Design," 2003 World Aviation Congress, Montreal, Society of Automotive Engineers, Paper 2003-01-3052, Sept. 2003.

[5] Mabey, D. G., "Buffeting Criteria for a Systematic Series of Wings," *Journal of Aircraft*, Vol. 26, No. 6, 1989, pp. 576–582. doi:10.2514/3.45805

[6] Ray, E. J., and Taylor, R. T., "Buffet and Static Aerodynamic Characteristics of a Systematic Series of Wings Determined from a Subsonic Wind Tunnel Study," NASA TND 5805, 1970.

[7] Isikveren, A. T., "Quasi-Analytical Modeling and Optimization Techniques for Transport Aircraft Design," Ph.D. Thesis, Royal Inst. of Technology, Dept. of Aeronautics, Stockholm, 2002, pp. 25–29.

[8] "Geometrical Properties of Cranked and Straight Tapered Wing Planforms," Engineering Science Data Unit, Rept. ESDU 76003, London, Jan. 1976; Amendment A, Oct. 1981.

[9] Anon., "A320-200 Technical Description," Airbus Industrie, Rept. 432 013/88, Issue 1, Toulouse, France, Mar. 1988.

[10] Anon., "Jet Transport Performance Methods," Boeing Flight Operations, Boeing Commercial Airplanes, Rept. D6-1420, 7th ed., Seattle, WA, May 1989.